



TITLE:

Crystallization Behavior of Normal Long Chain Compounds on a Uniaxially Drawn Film of Isotactic Polypropylene  
(Commemoration Issue Dedicated to Professor Ken-ichi Katayama On the Occasion of His Retirement)

AUTHOR(S):

Okihara, Takumi; Ohara, Masayoshi; Kawaguchi, Akiyoshi; Katayama, Ken-ichi

---

CITATION:

Okihara, Takumi ...[et al]. Crystallization Behavior of Normal Long Chain Compounds on a Uniaxially Drawn Film of Isotactic Polypropylene (Commemoration Issue Dedicated to Professor Ken-ichi Katayama On the Occasion of His Retirement). Bulletin of the Institute for Chemical Research, Kyoto University 1991, 69(2): 101-110

ISSUE DATE:

1991-09-14

URL:

<http://hdl.handle.net/2433/77382>

RIGHT:

## Crystallization Behavior of Normal Long Chain Compounds on a Uniaxially Drawn Film of Isotactic Polypropylene

Takumi OKIHARA\*, Masayoshi OHARA\*, Akiyoshi KAWAGUCHI\*  
and Ken-ichi KATAYAMA\*

*Received June 17, 1991*

The epitaxial modes of the long-chain compounds on a uniaxially drawn isotactic polypropylene (iPP) substrate were studied. They crystallized from the melt and by vapor-deposition onto iPP. In the case of crystallization from the melt, n-alcohol crystals grew with their (001) basal plane parallel to the substrate surface. The molecules were arranged with their chain axes normal or oblique to the surface. Carboxylic acids crystallized in monoclinic C- and C'-forms showed the epitaxial modes with the orientation analogous to that of the n-paraffin/iPP system. In crystallization by vapor-deposition, carboxylic acids did not show epitaxial growth, but n-alcohols exhibit several modes of epitaxial growth which are classified by the molecular orientation with respect to the iPP chain axis. Two modes of them are similar in that molecular chains of n-alcohols are parallel to the substrate surface; one has the same orientation as that in PE/iPP epitaxy, and in the other, molecular chains of n-alcohols are oriented parallel to the c-axis of the iPP substrate. The other modes have the same normal or oblique orientation as observed in the crystallization from the melt; flat-on lamellae grew.

KEY WORDS: Polypropylene/ Epitaxy/ n-Alcohols/ n-Carboxylic acids

### 1. INTRODUCTION

Epitaxial growth of long-chain compounds on the polyethylene (PE) substrate was reported in references.<sup>1,2)</sup> In the case of the polyethylene substrate, similarity of its crystal structure to the subcell of long-chain compound crystals has a decisive effect on epitaxial growth of the crystals. On the other hand, PE itself crystallizes on isotactic polypropylene (iPP) epitaxially.<sup>3,4)</sup> From these facts, it is expected that iPP could be a substrate for long-chain compound crystals to grow epitaxially on it. Really, epitaxial growth of n-paraffins on a uniaxially drawn iPP film took place.<sup>5)</sup> There were observed three types of epitaxial orientations where the molecular axes of n-paraffins were perpendicular to the substrate surface. The orientational relations were described in reference;<sup>5)</sup> type A<sub>1</sub> has the orientational relation of  $(001)_p // (010)_{iPP}$  and  $[110]_p // [001]_{iPP}$ , type A<sub>2</sub>  $(001)_p // (010)_{iPP}$  and  $[010]_p // [001]_{iPP}$  and type A<sub>3</sub>  $(001)_p // (010)_{iPP}$  and  $[110]_p // [001]_{iPP}$ . In addition, there is another epitaxial mode that molecular chains of n-paraffins lie parallel to the iPP substrate surface;  $(100)_p // (010)_{iPP}$  and  $[010]_p \nless 46^\circ [001]_{iPP}$ .

This orientational relation is the same as that in the epitaxy of PE/iPP system. This epitaxial mode was observed in n-paraffins with carbon number longer than 40. In this

\* 沖原 巧, 小原 正義, 河口 昭義, 片山 健一: The Institute for Chemical Research, Kyoto University, Uji, Kyoto-fu, 611 Japan)

paper, epitaxial growth of other long-chain compounds such as *n*-alcohols and *n*-carboxylic acids was studied. These compounds usually crystallize in a monoclinic or triclinic crystalline form and not crystallize in an orthorhombic form. Odd-numbered carboxylic acids crystallize in one or two of triclinic A', B' and monoclinic C'-forms depending on the chain length and crystallization condition.<sup>6-10)</sup> Even-numbered carboxylic acids crystallize in one or two of A-, B- and C-forms.<sup>11,12)</sup> *n*-Alcohols also crystallize in one or two crystalline forms of  $\alpha$ -,  $\beta$ - and  $\gamma$ -forms.<sup>13,14)</sup> These long-chain compounds are similar to *n*-paraffins in the chemical structure in that they have a long normal hydrocarbon chain and in the crystal structure in that their crystals have a similar orthorhombic subcell to that of *n*-paraffins; the subcell is the same as the unit cell of PE.<sup>15)</sup>

## 2. EXPERIMENTAL

Thin iPP substrate films for transmission electron microscopy were prepared by the method reported by Petermann and Gohil.<sup>16)</sup> iPP was supplied by Tokuyama Soda Co., Ltd. The experimental procedure to make specimens was as follows: a few drops of dilute solution of a long-chain compound were spread on the iPP film and the solvent was evaporated. Then, the film was heated above the melting point of the compound and cooled down to room temperature. The vapor-deposition crystallization was also applied. A thin iPP film and a long-chain compound were put in an evacuated chamber, and the compound was vapor-deposited onto the iPP substrate. Samples thus prepared were observed by a transmission electron microscope JEOL JEM-200CS. Long-chain compounds used in this study are *n*-paraffins with the carbon number 31 to 50, *n*-alcohols with the carbon number 17 to 30, *n*-carboxylic acids with the carbon number 17 to 30 and methyl and ethyl esters of some acids. They were purchased from Tokyo Kasei Kogyo Co., Ltd.

## 3. RESULTS

### 3.1. Crystallization from melt

When various kinds of *n*-alcohols were crystallized from the melt on the iPP drawn film, their crystals showed three different types of preferential orientations which are characterized by electron diffraction patterns shown in Figs. 1a, b and c. The patterns show  $hk0$  net patterns of *n*-alcohol crystals which superimposed on the iPP fiber pattern with a definite orientational relation to it. The presence of  $hk0$  net pattern indicates that molecular chains in *n*-alcohol crystals stand perpendicular to the iPP substrate in all three cases. In these cases, *n*-alcohols crystallized in the monoclinic  $\beta$ -form whose lattice parameter  $\beta$  (the unique angle of the unit cell) is 89°. Here, the molecular chains orient almost perpendicular to the substrate surface when the (001) plane is parallel to it. Odd-numbered alcohols crystallize in the  $\beta$ -form in a normal crystallization condition. Even-numbered alcohols are crystallized normally in  $\gamma$ -form. However, they crystallized in  $\beta$ -form on the iPP substrate. The above three orientations are distinguished in that the crystallographic *b*-axis of an *n*-alcohol make

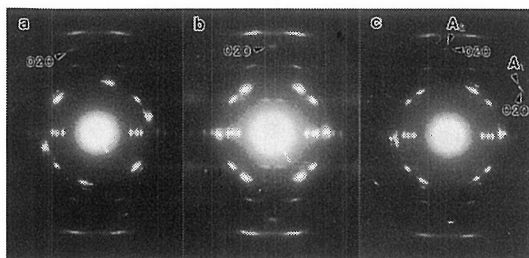


Fig. 1 Electron diffraction patterns of n-alcohol crystals grown on the uniaxially drawn iPP film. (a) 1-tetracosanol crystallized with mode  $A_3$ . (b) 1-triacontanol crystallized with mode  $A_2$ . (c) 1-tetracosanol crystallized with modes  $A_1$  and  $A_2$ .

different angles with the c-axis of the substrate. They are named  $A_1$ ,  $A_2$  and  $A_3$  according to the notation in epitaxy of n-paraffins on iPP,<sup>5)</sup> because the respective orientational relations of  $hk0$  net patterns are quite similar to those of corresponding epitaxial types for n-paraffins.

(1) Figure 1a shows the first type,  $A_3$ , which is observed most frequently. This type is identified by the feature that the 110 reflection from n-alcohol crystal coincides with the 111 reflection from the iPP fiber pattern. This mode of epitaxy has the same orientation as the mode expressed as  $A_3$  in reference<sup>5)</sup> for n-paraffins on iPP.

(2) The second type  $A_2$  is characterized by Fig. 1b. In this figure, the 200 reflection from n-alcohol crystal is on the equator of the iPP fiber pattern as described in reference,<sup>5)</sup> and in other words, the 020 reflection appears on the meridian of iPP.

(3) Figure 1c shows the third type  $A_1$ . This is less often observed. In this figure, the 110 reflection of an n-alcohol is on the equator of the iPP fiber pattern. This type of orientation was the same as type  $A_1$  of n-paraffins in reference.<sup>5)</sup>

Figure 2 shows an electron diffraction pattern of stearyl alcohol crystallized on a drawn iPP film. By measuring the lattice spacings, it is found that stearyl alcohol crystallized in the monoclinic  $\gamma_1$ -form. Since the molecular axis is oblique toward the  $a$ -axis, the dimension of  $a$  of the unit cell is larger than that of PE unit cell. The subcell of the  $\gamma_1$ -form is, however, orthorhombic and almost identical to the PE unit cell. In Fig. 2, the 020 spot of the n-alcohol is observed in the same direction with respect to the iPP fiber axis as in the case of the B mode of epitaxy of n-paraffins.<sup>5)</sup> In both cases,



Fig. 2 Electron diffraction pattern of stearyl alcohol crystals grown on the uniaxially drawn iPP film. Stearyl alcohol crystallized in  $\gamma_1$ -form.

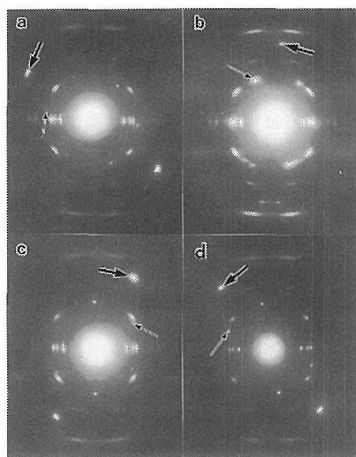


Fig. 3 Electron diffraction patterns of various n-carboxylic acid crystals grown from the melt on the uniaxially drawn iPP film. (a) n-nonadecanoic acid crystallized with mode  $A_{1m}$ . (b) n-tetracosanoic acid crystallized with mode  $A_{2m}$ . (c) n-nonadecanoic acid crystallized with mode  $A_{3m}$ . (d) stearic acid crystallized with mode  $A_{4m}$ .

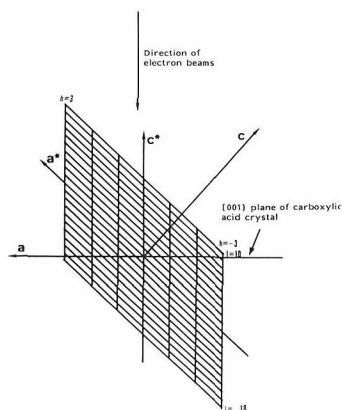


Fig. 4 Illustration for relation between the reciprocal lattice of a n-carboxylic acid crystal and incident electron beams.  $b$  and  $b^*$  axes are normal to the figure.

thus, the  $b$ -axis is in the same direction as regards the iPP fiber axis. The  $a$ -axis of the  $n$ -alcohol also lies parallel to the substrate surface, that is to say, the  $(001)$  plane is in contact with the iPP substrate surface.

Figure 3 shows typical electron diffraction patterns of various carboxylic acids crystallized on an iPP substrate. When most of carboxylic acids examined here, except for heptadecanoic acid, were crystallized on the iPP substrate from the melt or on the substrate kept at high temperatures by vapor-deposition, they showed one or more types of differently oriented overgrowth. The strong spots indicated with thick arrows are all indexed as  $020$ . Lattice spacings of weak spots indicated with a small arrows range from  $0.420\text{nm}$  to  $0.440\text{nm}$ . These are indexed as  $11l$  ( $l$  is dependent on the chain length, i.e. the kind of carboxylic acid). All diffraction patterns are interpreted on the basis of the Ewald construction for diffraction as shown in Fig. 4. The  $c^*$ -axis of the reciprocal lattice of a  $n$ -carboxylic acid is parallel to the incident electron beams. In this orientation, the  $020$  and  $11l$  reciprocal points are placed on the sphere of reflection at the same time. That means the  $(001)$  plane of the acid crystal is in contact with the iPP substrate. Even-numbered carboxylic acids crystallize in monoclinic  $C$ -form and odd-numbered carboxylic acid in  $C'$ -form. The molecular arrangement and inclination toward the  $a$ -axis in the  $C$ -form unit cells of the carboxylic acids is similar to that of  $n$ -alcohols with the  $\gamma_1$ -form, except for the magnitude of inclination angle  $\beta$  of molecules against the basal plane. In both kinds of crystals, their subcells are orthorhombic and the molecular packing in them is quite similar. Thus, these carboxylic

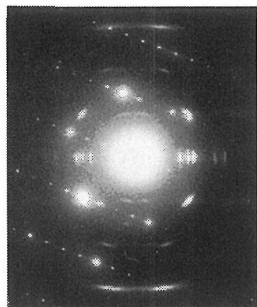


Fig. 5 Electron diffraction pattern of heptadecanoic acid crystallized from the melt on the uniaxially drawn iPP film.

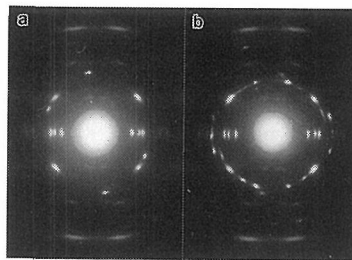


Fig. 6 Electron diffraction pattern of tetracosanoic acid ester crystal grown on the uniaxially drawn iPP film; (a) methyl ester and (b) ethyl ester.

acids and *n*-alcohols exhibit one or more types of oriented overgrowth characterized by electron diffraction patterns in Fig. 3. On the basis of the difference in the orientation of the 020 spot with respect to the fiber axis of iPP, the orientational modes distinguished by diffraction patterns in Figs. 3a, b, c and d are here denoted as  $A_{1m}$ ,  $A_{2m}$ ,  $A_{3m}$  and  $A_{4m}$ , respectively. According to the same notation as in the case of *n*-paraffins, A means that molecular chains stand on the substrate surface (not always perpendicular), the subscript *i* (*i*=1,2,3 and 4) denotes the same orientation of the *b*-axis as the corresponding subscript in *n*-paraffins do and *m* denotes that the crystalline form of carboxylic acids is monoclinic. Type  $A_{4m}$  shows the same orientation as described in the case of stearyl alcohol crystallized in  $\gamma_1$ -form (see Fig. 2).

Heptadecanoic acid crystallized in a different orientation from that of longer homologues. Its electron diffraction pattern is shown in Fig. 5. From the observed lattice spacings, it is found that all spot-like diffractions from the acid are indexed as  $0kl$ , i.e. the  $0kl$  net pattern superimposes on the fiber pattern of iPP. The figure is understood on the reflection condition that the electron beams are incident onto the acid crystals in the direction almost parallel to the *a*-axis, so that the  $0kl$  net pattern can be observed; the electron beams are incident horizontally (parallel to the *a*-axis) in Fig. 4. It is concluded that the (100) plane to which molecular chains align parallel is in contact with the substrate surface. Since the orientation of the  $0kl$  net pattern with respect to the iPP fiber axis differs from photograph to photograph, it seems that heptadecanoic acid does not crystallize epitaxially on the iPP substrate because of the shortness of molecular chain.

Other long-chain compounds showed epitaxial growth on the iPP substrate. Figure 6 shows electron diffraction patterns of methyl and ethyl tetracosanates crystallized on the iPP substrate from the melt. The crystal structures of these compounds are not reported, but the crystal structure of methyl stearate which has a subcell similar to that of *n*-paraffins is reported by Aleby.<sup>17)</sup> The crystallization behavior of methyl triacontanate on the (001) plane of KCl was reported by Ueda[18]. Though the crystal structure of this ester is also not analyzed yet, he has concluded that molecular chains of the methyl ester are perpendicular to the substrate, because his electron diffraction experiment showed the  $hk0$  net pattern of the subcell similar to that of *n*-paraffins and

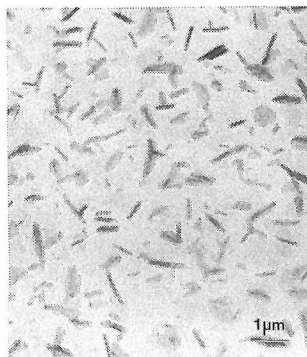


Fig. 7 Transmission electron micrograph of tetracosanoic acid crystals grown by vapor-deposition on a uniaxially drawn iPP film.

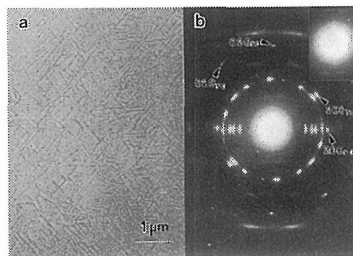


Fig. 8 (a) Transmission electron micrograph of n-triacontanol crystals grown on a uniaxially drawn iPP film and (b) the corresponding diffraction pattern. The inset is the enlarged pattern of the central part.

methyl stearate. In the present cases, the analogous  $hk0$  net patterns were observed, and hence, it is concluded that molecular chains stand perpendicular to the substrate. Further, since the  $hk0$  net pattern is oriented with respect to the fiber pattern in the same way as in the case of n-paraffins, epitaxial crystallization occurs.

### 3.2 Crystallization from the vapor phase

Figure 7 shows the morphology of vapor-deposited tetracosanoic acid on iPP kept at room temperature. Both edge-on and flat-on lamellae were observed and their orientation was random. It is likely that this vapor-deposition condition was not favorable for the carboxylic acid to crystallize epitaxially on the iPP substrate. In contrast to carboxylic acids, when n-alcohols were vapor-deposited on the iPP substrate at room temperature, they crystallized epitaxially. Figure 8 shows the morphology of n-triacontanol vapor-deposited on the iPP film at 25°C and the corresponding electron diffraction pattern. The pattern indicates that three types of epitaxial growth occurred on iPP. The presence of 001 reflections along the meridian of the iPP pattern indicates that molecular chains of the n-alcohol are parallel to the  $c$ -axis of the substrate. The others are flat-on lamellae grown epitaxially on the substrate. They are identified with two types of  $hk0$  net patterns of n-alcohol crystals which are definitely oriented with respect to the iPP fiber pattern. In them, the (001) plane of n-alcohol lamellae is in contact with the surface of the iPP substrate. Further, there is another orientation, though it is not recognized in Fig. 8b, in which orientation n-alcohol molecular chains take the same parallel orientation as those of PE chain do when PE crystallized epitaxially on iPP from the melt. All the types of epitaxy are distinguished by the difference of lamellar orientation on the substrate surface, as described in the case of crystallization from the melt. The epitaxial crystallization behaviors of n-alcohols are quite similar to those of n-paraffins.

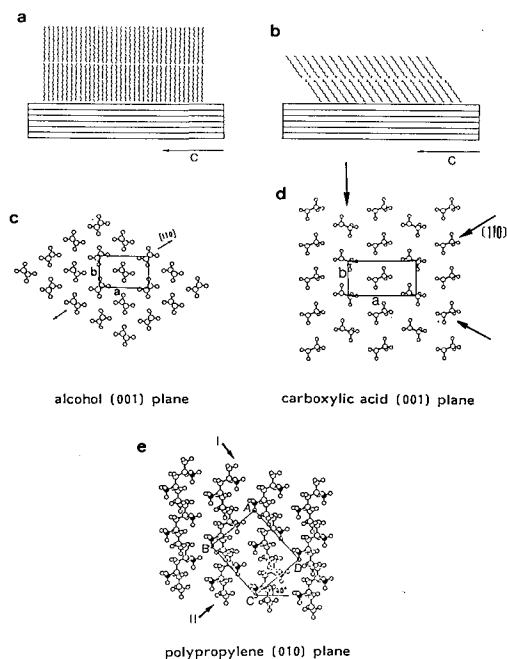


Fig. 9 (a) illustration of flat-on lamellar crystal of n-alcohol with  $\beta$ -form, (b) illustration of flat-on lamellar crystal of n-carboxylic acid, (c) molecular arrangement of (001) plane of n-alcohol crystal with  $\beta$ -form, (d) end methyl group arrangement of carboxylic acid crystal with C'-form and (e) molecular arrangement of polypropylene (010) surface. In (c), (d) and (e) large and small circles mean carbon atoms and hydrogen atoms, respectively. In (e), there is a rectangle ABCD which is a two-dimensional lattice of iPP (010) plane. The spacings of this lattice are as follows;  $AB=0.846\text{nm}$  and  $AD=1.005\text{nm}$ .

#### 4. Discussion

In the previous paper,<sup>5)</sup> we discussed the lattice matching in epitaxial growth of n-paraffins on iPP. In that case, the (010) plane of the iPP substrate plays an important role on epitaxy.

Figure 9a shows a model of the molecular orientation of the  $\beta$ -form of an n-alcohol crystallized epitaxially on the iPP substrate. The molecular chains are almost perpendicular to the substrate surface. In the case of crystallization of n-alcohols from the melt, they crystallized in  $\beta$ -form, but stearyl alcohol has another modification, that is,  $\beta$ -form. This result indicates that the  $\beta$ -form is favorable for the epitaxial growth of n-alcohols on iPP. Because the unique angle  $\beta$  of the unit cell is  $89^\circ$ , the crystal structure of the  $\beta$ -form is nearly orthorhombic and close to that of orthorhombic n-paraffins. Thus, the lattice matching similar to that of n-paraffin/iPP can be easily formed between n-alcohols with a  $\beta$ -form crystal and iPP. n-Alcohol molecules are dimerized in the crystal lattice by forming hydrogen bonds between -OH groups. It is



supposed that the coupled n-alcohol molecules behave in epitaxial crystallization as n-paraffins, because the end methyl groups are arranged in the same manner on the (001) plane as in the n-paraffin crystals. From the epitaxial crystallization behavior analogous to that of n-paraffins, it is considered that the contact plane with the iPP substrate is the (001) plane in which the end methyl groups are arranged as shown in Fig. 9c. It is stressed that the iPP (010) plane plays an important role on the  $A_3$  mode of epitaxy of n-paraffins. Here, it is most likely that the iPP (010) plane is in contact with the (001) plane of n-alcohols, realizing the following lattice coincidence. Figure 9e represents the molecular arrangement in the iPP (010) plane.<sup>5)</sup> Rows of end methyl groups shown by the arrows in Fig. 9c are parallel to the [110] direction. The interval between the rows is close to half of distance AB in Fig. 9e. Thus, the  $A_3$  epitaxial mode is achieved by fitting the end methyl rows of n-alcohols in the valleys between the side methyl rows on the iPP (010) plane.<sup>5)</sup>

From the electron diffraction, it is found that the (001) plane of the carboxylic acids was in contact with the iPP substrate and consequently, molecular chains are tilted on the substrate surface as modeled in Fig. 9b. Figure 9d shows the arrangement of end methyl groups on the (001) basal plane of carboxylic acid crystals of the C-form. In Fig. 9d, thin arrows indicate the direction in which end methyl groups align most densely. For examples, the interval between the rows of end methyl groups in the [110] direction is 0.436nm which is nearly equal to the (110) spacing of the orthorhombic n-paraffin cell (0.411nm).<sup>5)</sup> This spacing is in good agreement with half of the lattice spacing AB (0.846nm) shown in Fig. 9e. Thus, the row of end methyl groups in the (001) face of carboxylic acids fits in between two neighboring rows of side methyl groups in the iPP surface, as shown by the arrow I in Fig. 9e. Accordingly, the epitaxy mode  $A_{3m}$  is  $(001)_c // (010)_{iPP}$ , and  $[110]_c // [101]_{iPP}$  where c denotes a carboxylic acid. The distance AD in Fig. 9e is nearly equal to the dimension of  $a$  (twice of the interval between rows of end methyl groups aligned along the  $b$ -axis, as shown in Fig. 9d). The  $A_{1m}$  mode of epitaxy is caused as follows: the rows of end methyl groups fit in the valleys between the rows of side methyl groups in the (010) iPP surface oriented in the direction of the arrow II in Fig. 9e. The observed electron diffraction pattern of this epitaxy is explained on the basis of this orientation of carboxylic acids (see fig. 3a). In the case of  $A_{4m}$ , the  $b$ -axis of carboxylic acids is in the direction AD. Since the orientation with respect to the iPP fiber axis is the same as that in the B mode epitaxy of n-paraffins on iPP,<sup>5)</sup> this epitaxy occurs when carboxylic acid molecules lie down to fit in the channels running in the direction II. We should examine by energy calculation whether the epitaxy is energetically favorable or not. However, it is very difficult because too many atoms must be taken into consideration for the calculation. Analysis of  $A_{2m}$  is also difficult because there is no suitable lattice matching between the (001) plane of carboxylic acids and the (010) iPP plane for this mode of epitaxy, and again we must rely on the energy calculation to know this mode in detail. There are two problems in this epitaxy; one is whether this epitaxy is stable from the view point of interaction energy between carboxylic acids and the iPP substrate, and the other is which surface of the iPP substrate is assigned to this epitaxy, the (010) plane or any of others. So good explanation is not yet provided for  $A_{2m}$  mode epitaxy. Table 1 shows the grouping of

Table 1. Classification of epitaxial mode of long-chain compounds on the iPP substrate.

compound	epitaxial mode			
C <sub>17</sub> OH	A <sub>1</sub> ,	A <sub>2</sub>	A <sub>3</sub>	
C <sub>18</sub> OH ( $\beta$ -form)		A <sub>2</sub> ,	A <sub>3</sub>	
( $\gamma$ -form)				A <sub>4m</sub>
C <sub>23</sub> OH	A <sub>1</sub> ,	A <sub>2</sub> ,	A <sub>3</sub>	
C <sub>24</sub> OH	A <sub>1</sub> ,	A <sub>2</sub> ,	A <sub>3</sub>	
C <sub>26</sub> OH	A <sub>1</sub> ,	A <sub>2</sub> ,	A <sub>3</sub>	
C <sub>30</sub> OH		A <sub>2</sub> ,	A <sub>3</sub>	
C <sub>17</sub> COOH		A <sub>2m</sub> ,	A <sub>4m</sub>	
C <sub>18</sub> COOH	A <sub>1m</sub> ,	A <sub>2m</sub> ,	A <sub>3m</sub> ,	A <sub>4m</sub>
C <sub>23</sub> COOH	A <sub>1m</sub> ,	A <sub>2m</sub> ,	A <sub>3m</sub> ,	A <sub>4m</sub>
C <sub>25</sub> COOH	A <sub>1m</sub> ,		A <sub>3m</sub> ,	A <sub>4m</sub>
C <sub>29</sub> COOH	A <sub>1m</sub> ,	A <sub>2m</sub> ,	A <sub>3m</sub>	
C <sub>23</sub> COOCH <sub>3</sub>			A <sub>3</sub>	
C <sub>23</sub> COOC <sub>2</sub> H <sub>5</sub>		A <sub>2</sub> ,	A <sub>3</sub>	

epitaxial mode for long-chain compounds observed in melt crystallization.

In crystallization by vapor-deposition, carboxylic acid crystals did not show epitaxy on the substrate kept at room temperature (see Fig. 7). From this result, the epitaxial temperature of n-carboxylic acids seems to be higher than room temperature. In vapor-deposition crystallization of n-paraffins and n-alcohols, epitaxially oriented edge-on lamellae were observed on the iPP substrate at room temperature. Edge-on lamellae were not observed in the crystallization from the melt except for longer homologues. They take two orientations; one is explained by the B-mode epitaxy of n-paraffins on iPP,<sup>5)</sup> and the other is that molecular chains of long-chain compounds are parallel to the c-axis of iPP. In the latter, however, there is no lattice matching of a small misfit. Further accumulation of experimental data gives an explanation of this epitaxy.

Since the subcell of long chain compounds is the same as PE unit cell, their epitaxies on PE are performed to adjust a crystallographic plane of the subcell to the corresponding one of the PE unit cell. In the present long chain compound/iPP systems, the subcell also plays an important role. However, no subcell plane matches to "any of the lattice spacing on the (010) iPP surface" justly as in the long-chain compound/PE system. Consequently, a small misfit is inevitable. Because of this misfit, atoms or molecules placed near the interface can not occupy the stable position to form the stable crystal lattice of their own. As crystals grow, a lattice spacing gradually varies from the interface toward inside the crystal of the compound and reaches the value of the stable crystal lattice. Otherwise, to avoid this unstableness, the misfit dislocation is introduced at the interface. Though the epitaxially grown crystals remain unstable at the interface, their instability is eliminated by introducing the dislocation, and then they grow to be a stable form, maintaining the epitaxial orientation with the substrate.

The long-chain compound crystals which grew on the iPP substrate are in contact

with the substrate surface in a wide range. However, the lattice fitting between the crystal and the substrate could not be maintained over the entire interface. At the stage of nucleation, the orientational relation of the epitaxial growth is determined, i.e., this epitaxy is nucleation-controlled. A small contact area has an important role for epitaxial growth.

## REFERENCES

- (1) T. Okihara, A. Kawaguchi, M. Ohara and K. Katayama, *J. Crystal Growth*, **106** (1990)318.
- (2) T. Okihara, A. Kawaguchi, M. Ohara and K. Katayama, *J. Crystal Growth*, **106** (1990)333.
- (3) G. Broza, U. Rieck, A. Kawaguchi and J. Petermann, *J. Polymer Sci. Polymer Phys. Ed.*, **23** (1985)2623.
- (4) J. Petermann, G. Broza, U. Rieck and A. Kawaguchi, *J. Mater. Sci.*, **22** (1987)1477.
- (5) A. Kawaguchi, T. Okihara, M. Ohara, M. Tsuji, K. Katayama and J. Petermann, *J. Crystal Growth*, **94** (1989)857.
- (6) E. von Sydow, *Acta Cryst.*, **7** (1954)529.
- (7) E. von Sydow, *Acta Cryst.*, **7** (1954)823.
- (8) E. von Sydow, *Acta Cryst.*, **8** (1955)810.
- (9) E. von Sydow, *Acta Cryst.*, **8** (1955)845.
- (10) E. von Sydow, *Acta Chem. Scand.*, **9** (1955)1685.
- (11) E. von Sydow, *Acta Cryst.*, **8** (1955)557.
- (12) V. Vand, W.M. Morley and T.R. Lomer, *Acta Cryst.*, **4** (1951)324.
- (13) K. Tanaka, T. Seto, A. Watanabe and T. Hayashida, *Bull. Inst. Chem. Res. Kyoto Univ.*, **37** (1959)281.
- (14) S. Abrahamsson, G. Larsson and E. von Sydow, *Acta Cryst.*, **13** (1960)770.
- (15) C.W. Bunn, *Trans. Faraday Soc.*, **35** (1939)482.
- (16) J. Petermann and R.M. Gohil, *J. Mater. Sci.*, **14** (1979)2260.
- (17) S. Aleby, *Acta Cryst.* **15** (1962)1248.
- (18) Y. Ueda, *Bull. Chem. Soc. Jpn.*, **59** (1986)3775.